10

Laser processing of fused silica for fabricating microfluidic elements

© A.G. Bondarenko[1], R.A. Zakoldaev[1], A. Ramos Velazque[1,2]

[1] ITMO University,
197101 St. Petersburg, Russia
[2] LLC „Laser Center",
195067 St. Petersburg, Russia
e-mail: ag_bondarenko@itmo.ru

Received June 09, 2022
Revised June 16, 2022
Accepted June 30, 2022

The paper discusses the action of the power and the scanning speed of CO_2-laser radiation on the surface of fused silica for the manufacture of microchannels and microreservoirs for microfluidics tasks is investigated. The dependences of the size and the roughness of microstructures on of laser radiation parameters is established. The depth of microfluidic elements reaches $45\,\mu$m with a roughness of < 40 nm. The velocity of liquid propagation (up to 15 mm/s) is estimated for the microchannels fabricated. The wettability of microreservoirs is evaluated, with the wetting angle reaching $64 \pm 7^\circ$. The fabricated elements have a high transmission ($T \geq 0.8$) in the visible spectral range.

Keywords: CO_2-laser, microchannel fused silica, microfluidics.

DOI: 10.21883/EOS.2022.09.54833.3833-22

Introduction

Microfluidic (MF) elements find their application in scientific and engineering problems and, as a rule, are in great demand for creating lab-on-chip where it becomes possible to control fluid flows and distribute the volumes of reagents/analytes at the level of nano-pico-liters [1]. Particular attention is paid to the choice of material for the experiments with MF system. Quartz glasses can be considered universal in terms of high optical transparency, chemical resistance and lack of hygroscopicity. MF elements are predominantly formed on the surface of polymer materials by photolithography [2], and on the surface of quartz glasses by dry etching [3]. Then a polypropylene film is applied to the MF system to seal the system [4]. The key MF elements are microchannels for controlling and distributing liquid flows and microreservoirs for storing/mixing reagents and analytes [5]. However, these methods are multi-stage and resource-intensive, which makes it difficult to develop affordable and relatively cheap MF systems. Thus, the development of new methods and technologies for micromachining the surface of quartz glasses is an important direction of research.

The use of laser technologies for the processing of silicate materials, based on the resonant absorption of CO_2 laser radiation a promising direction in the development of MF elements. In the study [6], three main modes of the effect of CO_2 laser radiation on a SiO_2 matrix — densification matrices, ablation of nanometer layers per pulse and linear ablation of layers with a thickness of more than 150 nm per pulse. Thus, from a physical point of view, there are no obstacles to the implementation of MF elements with the required geometry. However, the methods for using commercial CO_2 laser systems for processing quartz glasses have not been amply developed yet, and namely, there seem to have been no studies on the permissible geometry of the formed structures, the roughness and thus, the wettability of the treated surface.

The present study is the first to discuss the technology of manufacturing MF elements — microchannels and microreservoirs on the surface of quartz glass using a commercial laser. For the recorded microchannels, the liquid propagation velocity has been estimated, and for the microreservoirs, the contact angles of wettability have been estimated. High optical transparency of the microreservoirs is confirmed by the transmission spectra in the visible range.

Experimental part

Laser microstructuring was carried out with a focused laser beam on the surface of quartz glass (JGS1). In the experiments, we used a C-Marker laser setup (LLC „Laser Center"), which generates radiation at a wavelength of $10.6\,\mu$m with a pulse repetition rate of 8 kHz. The laser beam was scanned using a galvanometric system of two mirrors, and the radiation was focused using a single-lens objective (SCAN 160/150-20 ST) with a focal length of 141 mm. The setup scheme is shown in Fig. 1, *a*. The size of the focal spot in terms of the $1/e$ level was $62\,\mu$m. The threshold energy for ablation of quartz glass in a pulse was $34\,\mu$J.

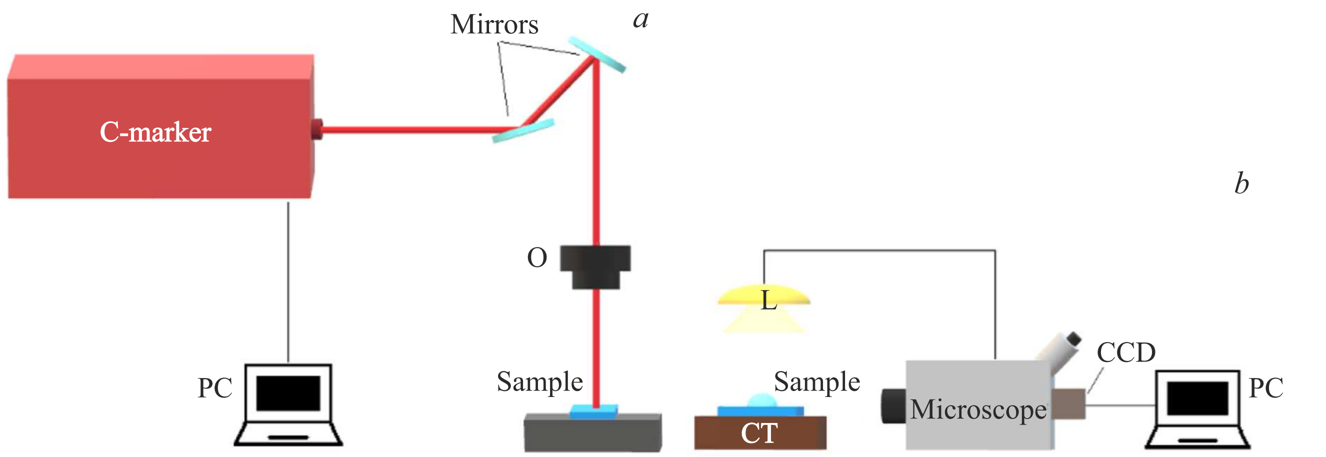

Figure 1. (*a*) Schematic representation of the C-Marker laser machine for glass processing: O — lens, PC — computer to control the laser machine. (*b*) Installation layout for measuring contact angles of wettability on a treated surface: PC — computer with ToupView software, CDD — ToupCam digital camera for surface visualization during measurements, CT — coordinate table, L — ring lamp.

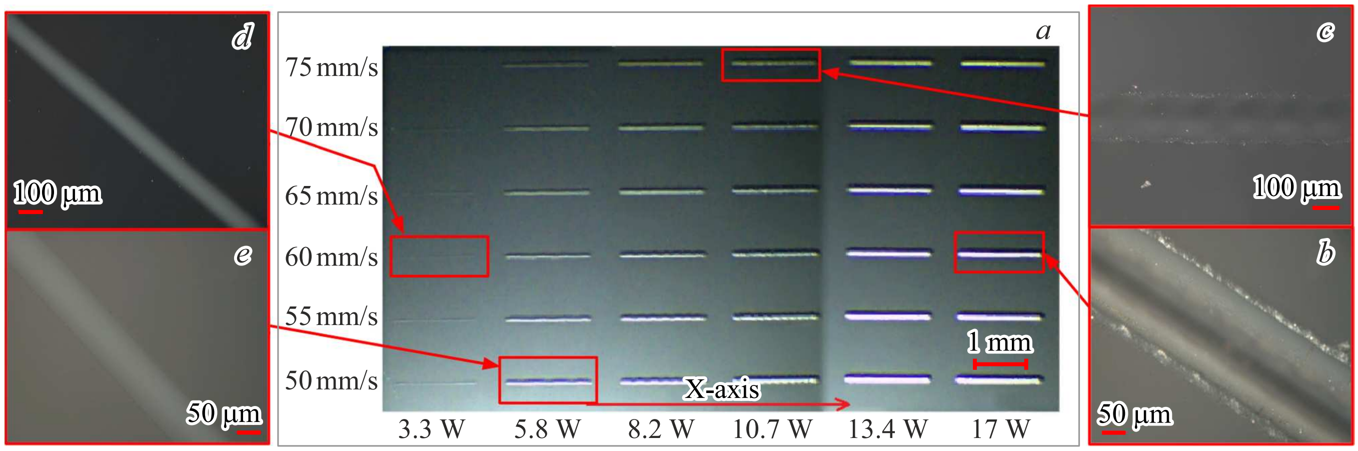

Figure 2. An array of microchannels on the surface of quartz glass and the laser processing conditions under which they were obtained (*a*), inhomogeneous microchannels with various defects (*b, c*) and homogeneous microchannels without stresses (*d, e*). The red frames show images of microchannels taken with a crossed polarizer and analyzer.

Microscopy was performed using a Zeiss optical microscope. To measure the dimensions and roughness of microstructures, a ZeScope optical profilometer and a Hommel Tester T8000 contact profilometer were used. The transmission spectra of fabricated microstructures in the visible range were measured with a LOMO microscope-spectrofotometer LOMO MSFU-K.

Wettability contact angles were measured to determine the wettability of the treated areas using an experimental setup including a LOMO microscope (1-4X), a ToupCam digital camera, an annular lamp, and a coordinate table (Fig. 1, *b*). Liquid was introduced into the channels by injecting and setting a drop of distilled water with a volume of 0.1 μl.

Results and discussion

Microfluidic channels

Figure 2, *a* shows photographs of microchannels formed on the glass surface at different values of the laser beam scanning speed and radiation power. The laser radiation power did not exceed 17 W (corresponding to the power density $q = 6 \cdot 10^4$ W/cm^2) in order to avoid the formation of stresses and cracks around the region impact (Fig. 2, *b*). The scanning speed is directly related to the overlap of laser pulses; therefore, it did not exceed 75 mm/s and provided an overlap percentage of 79–97%. A higher speed resulted in the discontinuity of the tracks (Fig. 2, *c*). The minimum track width was 46 μm (3.3 W, 75 mm/s). It can be seen from the photographs that the studied range of laser processing

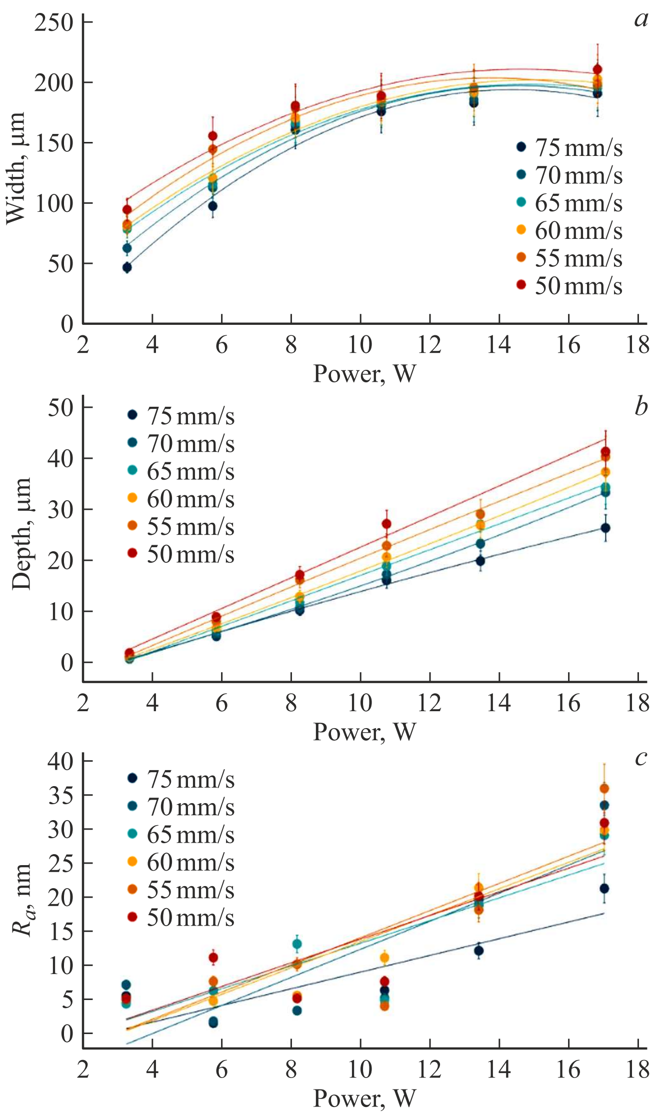

Figure 3. Dependence of the width (a), depth (b), and roughness Ra (c) of microchannels on the scanning speed and laser power.

parameters makes it possible to record homogeneous tracks (Fig. 2, *d, e*).

The track width can be accurately controlled by increasing the power, and the resulting dependence has a power-law character, where saturation occurs for widths of $190-210\,\mu$m (Fig. 3, *a*). In future research, it is possible to increase the track width by using a different focusing system or by processing in a converging beam.

The methods of contact profilometry were used to study the roughness and the depth of the tracks formed. For example, the dependence of the track depth on the laser radiation power at a constant scanning speed is shown in Fig. 3, *b*. The function is linear with the coefficient $R^2 = 0.98$. It can be assumed that a further increase of the depth can be obtained by progressive scanning without increasing the power of laser radiation. In the present study, the track depth can be set in the range of $0.5 \pm 0.1-45 \pm 6\,\mu$m. The behavior of the curve agrees well with the study [7] that discusses the dependences of the depth of craters on the energy density of CO_2 laser radiation during pulsed ablation of quartz glass.

For microfluidics problems, besides the channels geometry, it is very important to control their roughness, for example, the parameter R_a. Increased roughness reduces friction, which can result in an increase in fluid flow velocity in microchannels [8]. An increase in roughness is noticeable with a decrease in the scanning speed (Fig. 3, *c*).

At the next stage, the liquid was deposited on one side of the channel. For test channels, a mode was chosen that provides recording of a track with a depth of $8.5\,\mu$m and a roughness of 11 nm. When $0.1\,\mu$l of distilled water was deposited on one side of the channel, the liquid spread along the entire length of the channel (Fig. 4, *a*). It should be noted that potentially a channel with a length of 6 mm contains a volume of liquid ~ 7.5 nl. The moment of drop settling is shown in Fig. 4, *b*; after 0.16 s, a directed propagation of the liquid along the created track formed is observed. After 1.5 s, the liquid is uniformly distributed within the channel (Fig. 4, *c*). In further, we can envisage using a smaller volume of liquid. The microchannels formed can be used for an MF system based on quartz glass. Furthermore, we were able to estimate the rate of liquid flow through several microchannels depending on their roughness (Fig. 4, *d*). The speed varies within 4.15 mm/s, which is 5 times faster than similar MF channels on glass [9].

Microreservoir

Microreservoir, is another key MF element, which can be implemented by this technology with line-by-line overlapping of tracks. However, to record microreservoirs with overlapped tracks, the laser processing parameters had to be adjusted. Thus, the microreservoirs were recorded on glass with varying laser radiation power (3.3–5.8 W) and varying percentage of overlap along the Y axis (75–95%) (Fig. 5). The values of the depth and roughness of the microreservoirs were obtained with optical and contact profilometers.

Dependences of microreservoir sizes on laser radiation parameters showed an increase in the depth $(1 \pm 0.5-35 \pm 5\,\mu\text{m})$ and in the roughness S_a $(150 \pm 15-4500\ pm100\,\text{nm})$ when the overlap of the laser spot along the Y axis increases from 75 to 95%.

The microreservoirs formed were also tested with distilled water $(0.1\,\mu\text{l})$ deposited to determine the contact angle of wetting. For microreservoirs, we plotted the dependence of the contact wettability angles against the roughness parameter S_a, taking into account the percentage of laser spot overlap and the laser processing parameters (Fig. 6).

The graph clearly shows that the contact angles of wettability increase linearly as the parameter Sa increases. This

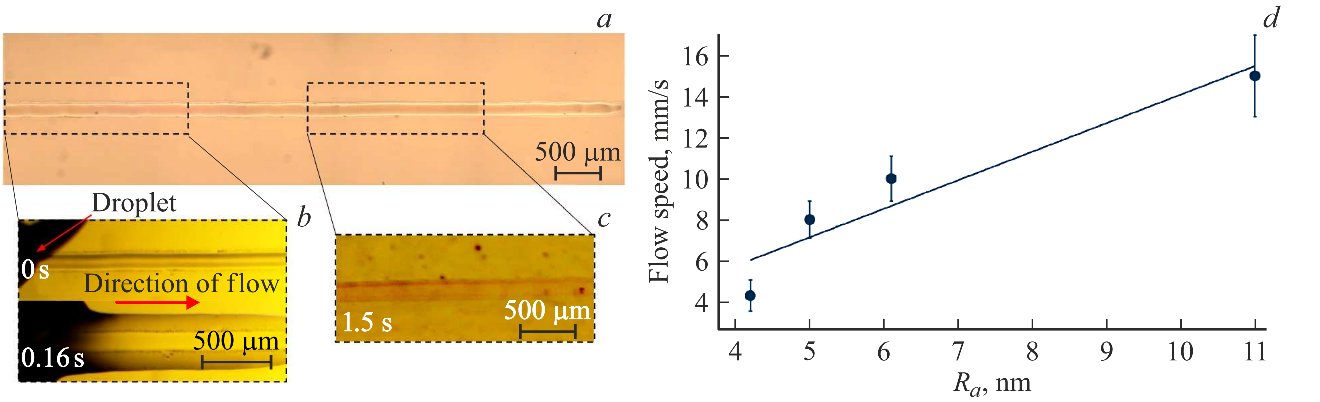

Figure 4. Microchannel tested for the deposition of a drop of distilled water (a), propagation of a liquid drop along the microchannel (b, c) and dependence of the flow velocity on microchannel roughness Ra (d) .

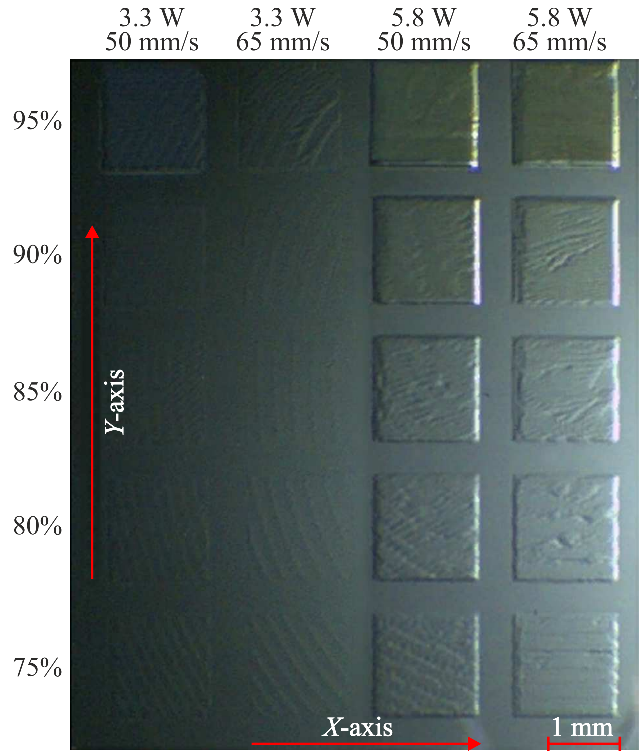

Figure 5. An array of microreservoirs on the surface of quartz glass and the laser processing conditions under which they were obtained.

is probably due to the fact that the obtained microstructures with high roughness values follow the Wenzel model [10], which describes the behavior of rough surfaces with low wettability.

Transmission spectra

The transmission spectra of the microreservoirs studied in the visible range (400–800 nm) are shown in Fig. 7. The untreated quartz glass surface exhibits high transmission (transmittance $T \sim 0.93$).

The fabricated microstructures have a higher roughness, which results in a decrease in the transmittance to $T = 0.8$ in the blue-green region of the spectrum.

Conclusion

This study has been the first to demonstrate the possibility of fabricating MF structures of various geometries on the surface of quartz glass using radiation from a commercial CO_2 laser. the dependences of their sizes and roughness on the parameters of laser processing were derived for the resulting microstructures,. The investigated microchannels demonstrate the movement of a liquid at a speed of 4–15 mm/s as well as an increase in the values of contact wetting angles for microreservoirs with increasing S_a. The results of spectroscopy show a decrease in the transmission of microreservoirs to $\sim 80\%$.

Funding

This study was supported financially by the NIRMA grant of PT MF of ITMO University.

Acknowledgements

A.G. Bondarenko thanks „Laser Center“ for providing the necessary equipment for the experiments.

Conflict of interest

The authors declare that they have no conflict of interest.

References

[1] M. Hitzbleck, E. Delamarche. Chem. Soc. Rev., **42** (21), 8494-8516 (2013). DOI: 10.1039/C3CS60118H

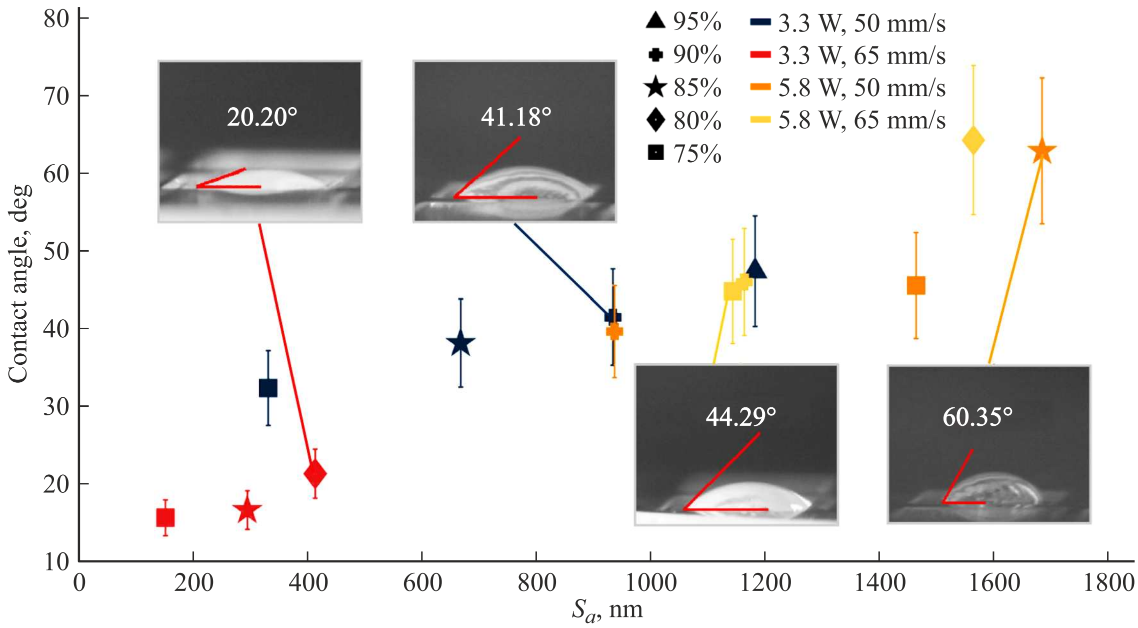

Figure 6. Dependence of the wettability contact angles on the roughness Sa of microreservoirs at various laser processing parameters.

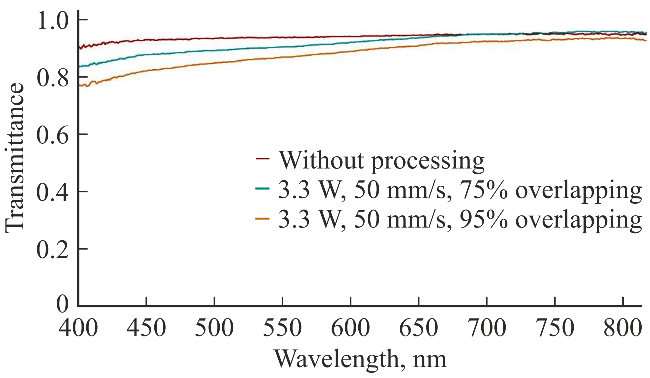

Figure 7. Transmission spectra of the surface of untreated quartz glass and obtained microreservoirs.

[2] A.E. Mironov, J. Kim, Y. Huang, A.W. Steinforth, D.J. Sievers, J.D. Eden. Nanoscale, **12** (32), 16796–16804 (2020). DOI: 10.1039/D0NR04142D

[3] M.J. Ahamed, D. Senkal, A.A. Trusov, A.M. Shkel. In: SENSORS (IEEE, 2013), p. 1–4. DOI: 10.1109/icsens.2013.6688574

[4] T. Wang, J. Chen, T. Zhou, L. Song. Micromachines, **9** (6), 269 (2018). DOI: 10.3390/mi9060269

[5] J. Choi, R. Ghaffari, L.B. Baker, J.A. Rogers. Sci. Adv., **4** (2), (2018). DOI: 10.1126/sciadv.aar3921

[6] A. Temmler, C.B. Weingarten, B. Schober, E. Uluz. Applied Surface Science, **555**, 149609 (2021). DOI: 10.1016/j.apsusc.2021.149609

[7] K.M. Nowak, H.J. Baker, D.R. Hall. Applied optics, **54** (29), 8653–8663 (2015). DOI: 10.1364/AO.54.008653

[8] A.S. Rawool, S.K. Mitra, S.G. Kandlikar. Microfluidics and nanofluidics, **2** (3), 215–221 (2006). DOI: 10.1007/s10404-005-0064-5

[9] Y. Zhu, K. Petkovic-Duran. Microfluidics and Nanofluidics, **8** (2), 275–282 (2010). DOI: 10.1007/s10404-009-0516-4

[10] E. Bormashenko. Advances in colloid and interface science, **222**, 92–103 (2015). DOI: 10.1016/j.cis.2014.02.009